2013 International Conference on Electrical Machines and Systems, Oct. 26-29, 2013, Busan, Korea

Thermal Modeling as a Tool to Determine the Overload Capability of Electrical Machines

Sara Mahdavi, Thomas Herold, Kay Hameyer
Institute of Electrical Machines, RWTH Aachen University
E-mail: sara.mahdavi@iem.rwth-aachen.de

Abstract —Temperature is a key parameter in designing electrical machines. Common models that are used for the calculation of the temperature inside the machine's components can be considerably complicated. Depending on the application of the electrical machine, a certain level of accuracy in the model must be achieved. This work provides a basic guideline for modeling the thermal behavior of electrical machines especially for the applications with varying load conditions. Since temperature measurements for various working points of the electrical machines is very time consuming, usage of the thermal model to simulate the temperatures can be time saving. Moreover, a precisely parameterized thermal network can be used as a tool for designing similar machines to achieve higher power densities.

I. Nomenclature

List of the symbols used in this work is as following:

Symbol	Description
A	Area in m^2
α	Heat transfer coefficient in $m^{-2}\cdot K^{-1}$
λ	Specific thermal resistance in $W\cdot m^{-1}\cdot K^{-1}$
C	Thermal capacitance in $W\cdot s\cdot K^{-1}$
c	Specific heat capacity in $W\cdot s\cdot K^{-1}\cdot Kg^{-1}$
l	Length in m
m	Mass in kg
P	Power in W
r	Radius in m
R	Thermal resistance in $K\cdot W^{-1}$
ρ	Mass density in $kg\cdot m^{-3}$
t	Time in s
T	Temperature in K
V	Volume in m^3
W	Energy in W·s

II. Instroduction

Approximately 35% of malfunctions in electrical machines are due to winding failures. Stator winding's insulation is the dominant electric component that is statistically responsible for motor faults [1]-[4]. In order to guarantee a specific life time based on the thermal aspects of the winding for electrical machines, the temperature of the winding may not exceed a maximum allowed value [4]. On the other hand temperature, which is related to the winding's maximum allowable current, is also a power limiting parameter. The output torque and power of electrical machines are proportional to the air gap flux density as well as the current density inside the windings. These two factors are limited by the maximum allowable temperature of the winding depending on its standardized insulation class. Electrical machines are usually designed for continuous operation and a life time of approximately 20,000 hours of operation [5]. Based on this life time for continuous operation, various dynamic drive cycles can be adapted to still guarantee the projected life time. Standard [5] refers to this condition and the conventional design strategies are oriented towards the standard guidelines. However, if a motor's expected life time is considerably shorter, e.g. 6,000 to 8,000 hours of operation for a household device or an electrical vehicle, using the conventional design methods will result into a machine that is thermally over dimensioned. In this study and according to the information that the proposed thermal model provides, the maximum allowed temperature and therefore the output power can be increased above its nominal assigned data for the continuous operation with 20,000 hours of life time. This allows a thermally optimized operating strategy in electrical machines which allows an economical utilization of natural resources. The thermal network of the parameterized machine in this work can be adjusted in terms of geometrical dimensions to estimate the temperature in other electrical machines. The thermal model, estimating relevant temperatures in the machine, is described in the next chapter.

III. Thermal Network Modeling and Parameterization

Thermal Network models provide the transient temperature estimation in electrical machines. These models consist of:

1) **Thermal sources**, which represent the copper, iron, bearing, air gap and other losses.

2) **Thermal resistances**, which represent the heat propagation paths in the machine.

3) **Thermal capacitances**, which represent the thermal energy storage inside the machine components (windings, laminations, housing etc.).

The values of the resistances and capacitances depend on the dimensions of the machine components and the used materials.

Fig. 1 provides an example of a thermal network inside the stator yoke of an asynchron machine.

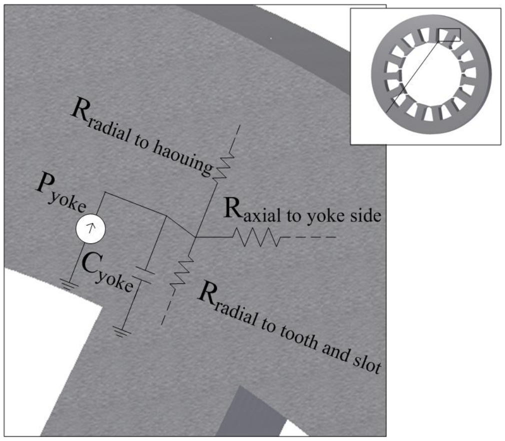

Fig. 1. Thermal network model of stator's yoke.

In a cylindrical coordinate system the heat paths (thermal resistance) and heat storage elements (thermal capacitance) are described by (1)-(4) for stator yoke.

$$R_{radial\ to\ cooling} = \frac{1}{4\pi \cdot \lambda_{stator-radial} \cdot l_{fe}} \left(1 - \frac{2 r_2^2 \ln(\frac{r_1}{r_2})}{r_1^2 - r_2^2} \right) \quad (1)$$

$$R_{radial\ to\ tooth\ and\ slot} = \frac{1}{4\pi \cdot \lambda_{stator-radial} \cdot l_{fe}} \left(\frac{2 r_1^2 \ln(\frac{r_1}{r_2})}{r_1^2 - r_2^2} - 1 \right) \quad (2)$$

$$R_{axial\ to\ yoke\ side} = \frac{l_{fe}}{12\pi \cdot \lambda_{stator-axial} \cdot (r_1^2 - r_2^2)} \quad (3)$$

$$C_{yoke} = c_{stator} \cdot \rho_{stator} \cdot \pi \cdot \left(r_1^2 - r_2^2 \right) \cdot l_{fe} \quad (4)$$

In (1) to (4) the symbols are:

r_1 and r_2: the outer and inner yoke radii,
l_{fe}: the iron stack length,
$\lambda_{stator\text{-}axial}$, $\lambda_{stator\text{-}radial}$: the specific thermal resistances of stator laminations in axial and radial direction,
c_{stator}: the specific capacity of stator lamination and
ρ_{stator}: the mass density of stator lamination.

More details and explanations about modeling thermal paths inside machines are available in [6]-[9], [20]. Heat conduction and heat transfer inside the machine are graphically illustrated in Fig. 2 and Fig. 3. Copper losses can be calculated by means of analytical methods while iron losses can be calculated by FE-models. For the calculation of air and bearing friction losses empirical formulas [10]-[11] can be applied. The yoke network (see Fig. 1) is expanded in this work to include all the components of the electrical machine (stator teeth, winding, rotor laminations, etc.). The equivalent thermal network consists of 34 nodes and 62 thermal resistances

The thermal network consists of numerous loss sources, resistances and capacitances. Steady state temperature in any position inside the electrical machine is dependent on the generated local losses inside the machine ($P_1 \ldots P_n$ in Fig. 1 as well as the heat distribution paths inside the machine ($R_1 \ldots R_k$). Heat storage inside the machine is responsible for the transient temperature progression inside the machine. This characteristic is represented by thermal capacitances ($C_1 \ldots C_p$). The thermal capacitances are responsible for the time dependent temperature behavior of the machine. From a mathematical point of view all materials have thermal capacitances. Nevertheless for practical applications the thermal capacitances of some components are negligible compared to the others. The specific heat capacity of the commonly used materials in electrical machines is available in chapter VIII.

TABLE I presents the saved thermal energy in the asynchron machine under study (see V), when the rotor is fixed at stand still, coolant of the water jacket cooling has 25°C at machines input and the stator has nominal current at 0.1 Hz. In that case different components of the machine are each heated up to a specific temperature. Knowing the mass of each component, its stored energy can be calculated. It can be seen that most of the energy is stored in metallic parts and impregnation. Hence, the thermal capacitance of the air encapsulated by the machine can be neglected.

TABLE I
Stored thermal energy in the asynchron machine when rotor is fixed at stand still and the machine is fed with nominal current at 0.1Hz.

Material	**Stored thermal energy compared to the stored thermal energy in copper**
Winding and rotor bars	100%
Air	0.01%
Laminations	288.2%
Aluminum housing	74.4%
Impregnation	12.3%

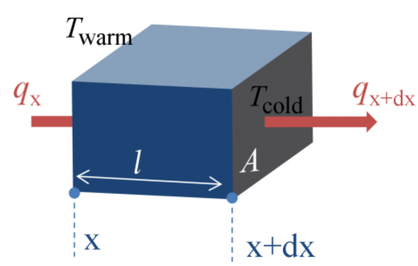

Fig. 2 Heat flow in a block.

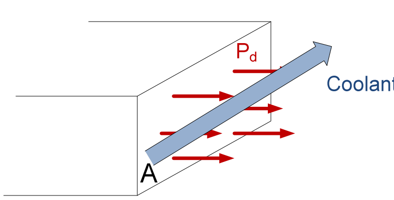

Fig. 3 Heat transfer from the hot surface to coolant due to convection.

IV. Thermal Network and Its Operating Point Dependency

Since the winding's temperature is directly related to electrical machines' expected life time, the accuracy of the thermal model is important. This dependency is described by the *Montsinger's* rule [16] as follows: Increasing the continuous state temperature of the insulation by 10 K reduces its life time by half. To assure the model's accuracy, the analytically parameterized thermal network has to be validated and calibrated by measurements. The reason for calibrating the analytically parameterized network is the following:

1) Depending on the operating point of the machine, the parameters (R, C and P) may change. It means that the thermal network has a dynamic nature and neglecting this characteristic can result into simulation results that show deviations from the reality in different operating points. For instance, ohmic copper losses inside the winding change with increasing the temperature because, the electric resistance of copper increases with temperature.

2) The parameterization is based on the values (of the specific heat density and specific thermal resistance) that can be found in the literature [10]-[14]. These values are defined within a spectrum, e.g. the specific heat resistance of the windings impregnation can change depending on the type and amount of the used impregnation material as well as the impregnation method. Hence a purely analytical approach for parameterizing a thermal network is not sufficient and an experimental investigation of the specific heat resistance of the machine parameters is necessary. Fig. 4 presents a structured methodology to calibrate the thermal network model and assure its accuracy as a dynamic model. If only one operating point of the electrical machine is of interest, there would be N possible combinations of $R_1 \ldots R_k$ that can fulfill the temperature equation. For instance the specific thermal resistance of paper (which is used as the slot insulation) varies between 0.05 and 0.23$\mathrm{W \cdot m^{-1} K^{-1}}$ [14], depending on the paper type and the local temperature. Knowing this spectrum, a sensitivity analysis can be performed to find the deviations in temperature depending on the changes in the thermal resistances. This analysis helps with the following:

1) Deviation bandwidth of the analytically calculated thermal network can be estimated. For instance, the maximum deviation of the enwinding temperature is 18.1% and the maximum deviation of the bearings temperature is 29.2%.

2) Those R values that affect temperatures the most can be identified. In case of a deviation between the measurement and analytically calculated model, one can change the resistances within their physically meaningful spectrum in a way that the local temperatures that differ from the measurement have the smallest deviation. For instance, the temperature in enwinding is very sensitive to the thermal resistance between the endwinding and water jacket cooling (threw the air) as well as the thermal resistances of the winding's insulations materials.

V. Test Setup

The shaft of the test squirrel cage machine is connected to a stand still wheel cylinder which does not allow any movement of the rotor. During the test the machine is cooled with a cooling medium that has 25ºC input temperature and flows with a mass rate of 6 lit/min. The machine arrangement is on an iron machine bed. A three phase 0.1 Hz sinusoidal current is injected in the stator windings and the input power to the machine is measured with a power analyzer. The results of the test as well as the adjusted thermal network's simulations are presented in Fig. 5. The machine bed consists of 835 kg flat massive cast iron with several tracks. Due to its mass and considerable surface, the machine bed limits the maximum temperature of the electrical machine.

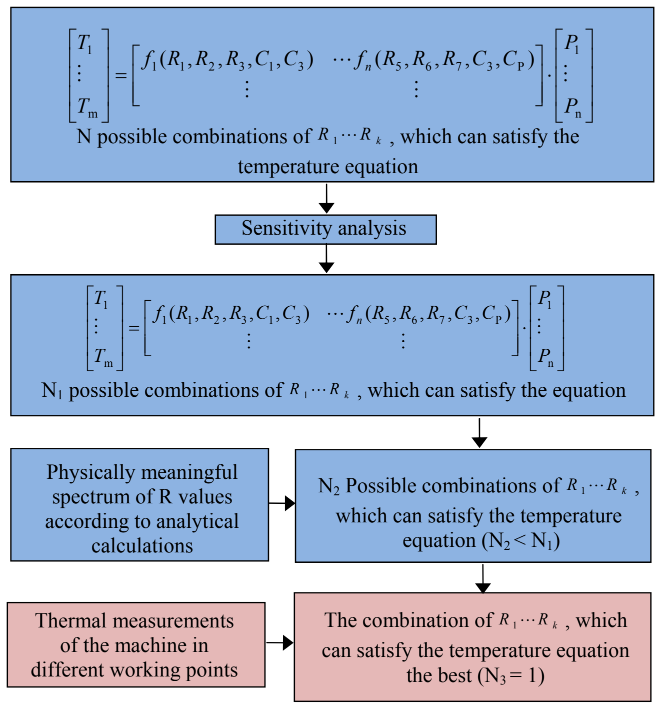

Fig. 4 Methodology for the calibration of the thermal network: simulated temperatures: $T_1 \ldots T_m$, model resistances: $R_1 \ldots R_k$, model capacitances: $C_1 \ldots C_p$, model loss sources: $P_1 \ldots P_n$.

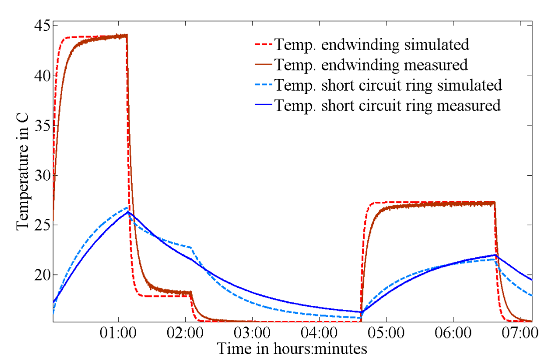

Fig. 5 Simulated and measured temperature of the enwinding and short circuit ring of the asynchron machine (Nominal current flows in the winding, rotor is at stand still, cooling medium has a mass rate of 6 lit/min and has 25°C temperature at machine's input).

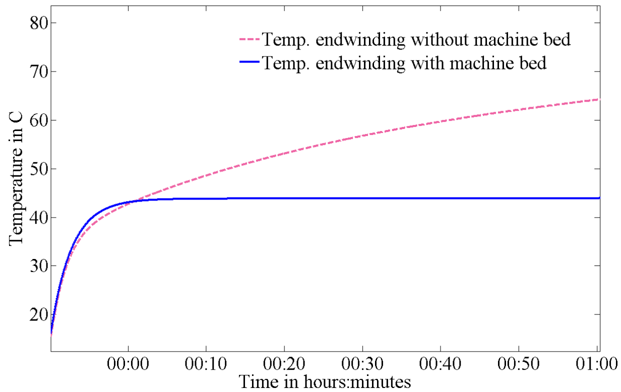

Fig. 6 Simulated end winding temperature with and without machine bed in the asynchron machine (Nominal current flows in the winding, rotor is at stand still, cooling medium has a mass rate of 6 lit/min and has 25°C temperature at machine's input).

From the thermal network point of view, the machine bed introduces a considerable amount of thermal capacitance (due to its mass) as well as thermal resistance (due to radiation and convection from its surface to ambient) to the whole thermal network. Nevertheless the tested electrical machine can be installed on an arbitrary machine bed or it can be connected to a chain of other devices such as planetary gears. Hence it is important to know the machine's thermal behavior in absence of the machine bed. Performing measurements on the machine in absence of machine bed is due to technical reasons not possible. Hence the machine was simulated in absence of the machine bed. The results are presented in Fig. 6.

This result is of major importance for machine applications with changing loads (e.g. tooling machines and electrical vehicles). This simulation shows that at least the transient output power of these machines can be increased with respect to the devices (planetary gears, metallic arms, etc.) that are connected to them.

VI. Selection of the Operating Point

In order to verify the thermal network it is important to inject the losses in the machine that are precisely calculable and their location is known. Hence, the machine should be operated in a way that there are as less iron losses produced as possible. The first possibility is to connect a DC current to the machine. This way, no iron losses are produced. Nevertheless since the machine is star connected and its star point is not accessible, it is not possible to generate the same amount of losses in all three phases and the machine would not have a symmetrical heat generation in all three phases.

TABLE II
Distribution of local losses in asynchron machine when rotor is braked and stator frequency is 0.1 Hz and machine is cooled with a coolant of 25°C at machine input.

Stator current	**Iron losses in stator and rotor (FE calculated)**	**Copper losses in stator (analytically calculated)**	**Ohmic losses in Rotor bars and short circuit ring (FE calculated)**
I=115A	<0.24W	419.54W	19.35W
I=78A	<0.24W	350.89W	15.31W
I=35A	<0.24W	72.87W	5.27W

In order to solve the temperature equation, the thermal coupling between the three phases has to be considered. This asymmetry introduces more complexity to the system. The solution used in this work is to inject a low frequency three phase current to the system. Frequency of 0.1 Hz was chosen. The rotating field produced by this three phase current will induce the stand still rotor as well as stator with 0.1 Hz frequency. This frequency is comparably smaller than the nominal rotor slip frequency (which is 1 Hz). Hence the iron losses due to this frequency are neglectable. This assumption is validated via calculations in iMOOSE finite element software [22]. Results are listed in TABLE II.

VII. Conclusions and Outlook

This work proposes a general methodology for the implementation of a thermal model that can be applied to utilize the thermal capacity of electrical machines depending on the load spectrum. Thermal measurements for every operating point can take hours depending on the machine type while the usage of the thermal model takes less than a minute. The thermal model is parameterized according to the machine's geometry and the specific thermal resistance of the materials inside it. The specific heat resistances vary within a spectrum according to the literature [6]-[14]. Sensitivity analysis is performed to find the model's temperature deviations and possible thermal resistance values. The model is then calibrated according to measurements. The thermal resistances are altered within their physical possible spectrum to derive the thermal network that fits the measurements best. Thermal measurements are performed while the rotor is at stand still and iron losses are negligible. Measured and simulated results are presented in Fig. 5 and Fig. 6 for comparison. The influence of the surrounding is another discussed aspect in this work. In Fig. 6 it is shown that the electrical machine has a significantly different thermal behavior with and without the machine bed. These results could be useful in thermal design and optimization of electrical machines that are connected to various devices. The resulting model in combination with dynamic life time estimation [15], [18] may increase power density of the machine depending on the expected life time.

Thermal measurements could also be performed with DC currents. Nevertheless since the star point of motors are usually not accessible, DC currents cause nonsymmetrical stator heating. In the normal operation of electrical machines, all three phases are heated up symmetrically; hence the thermal coupling between the three phases does not play a role. Nevertheless if the machine is fed by DC currents the thermal coupling between the three phases needs to be considered or some other methods need to be applied. Parameterization with DC currents will be the subject of the upcoming works.

VIII. Appendix

The specific density of the commonly used materials in electrical machines is listed in TABLE III.

TABLE III
specific heat density in different materials [10]-[14].

Material	**Specific heat density** *c* **in Ws/ (kg· K)**
Air	1065 (50°C)
Copper	380(50°C)
Iron	502(50°C)
NdFeB	440(20°C)
Aluminum	900 (20°C)
Epoxy resin	1100(50°C)

The specific thermal resistances of the commonly used materials in electrical machines are listed in TABLE IV.

TABLE IV
Specific thermal resistances in different materials[10]-[14].

Materiel	**Specific thermal resistance λ in W/K**
Copper	372…393
Aluminum	203…240
Air	0.024…0.029
Unsaturated Polyester	0.2
Lamination	24…60
Glass	0.5 …1.36
EBG.NO20	38
NeFeB	7500
Carbon fiber	0.5
Mylar film	0.2
Epoxy-resin	0.17 …0.44
Brass	64…128
Lead	35
Bronze	58
Iron	51…70
Wood	0.17
Paper	0.05…0.23
Oxygen	0.237
Vacuum	0
Hydrogen	0.119…0.17
Water	0.54…0.643
NdFeB	9
SmCo	12
Ferrite	2…6
AlNiCo	10…120

REFERENCES

[1] P. Zhang, Y. Du, T. Habetler, B. Lu "A Survey of Condition Monitoring and Protection Methods for Medium-Voltage Induction Motors," *IEEE Transactions on Industry Applications*, vol.47, pp. 34-46, Jan.- Feb. 2011.

[2] P. O'Donnell, "Report of Large Motor Reliability Survey of Industrial and Commercial Installations, Part I", *IEEE Transactions on Industry Applications*,1985.

[3] P. O'Donnell, "Report of Large Motor Reliability Survey of Industrial and Commercial Installations, Part II", *IEEE Transactions on Industry Applications*,1985.

[4] P. O'Donnell, "Report of Large Motor Reliability Survey of Industrial and Commercial Installations, Part III", *IEEE Transactions on Industry Applications,* 1987.

[5] IEC 60034-1, "Rotating electrical machines – Part 1: Rating and performance", International standard edition 11, 2004.

[6] G. C. Montanari, "Progress in Electrothermal Life Modeling of Electrical Insulation During the last Decades," *IEEE Transactions on Dielectrics and Electrical Insulation*, vol. 9 pp. 370-745, Oct. 2002.

[7] Z J Liu, D Howe, P H Mellor, M K Jenkins, "Thermal analysis of permanent magnet machines" *IEEE Sixth International Conference on Electrical Machines and Drives,* 1993.

[8] R. Wrobel and P. H. Mellor , "A General Cuboidal Element for Three-Dimensional Thermal Modelling" *IEEE Transactions on magnetics*, 2010.

[9] Aldo Boglietti, Andrea Cavagnino, Mario Lazzari, and Michele Pastorelli , "A simplified Thermal Model for variable Speed Self-cooled Induction Motor*", IEEE Transactions on Industry Applications*, 2003.

[10] J. Sari, "Thermal analysis of high speed induction machines", Dissertation, Helsinki university of technology, 1998.

[11] J. Lindstroem, "Thermal Model of a Permanent-Magnet Motor for a Hybrid Electric Vehicle", Department of Electric Power Engineering , Chalmers University of Technology Goeteborg, Sweden, Report , April 1999.

[12] P.H. Mellor, D. Roberts, "Lumped parameter thermal model for electrical machines of TEFC design", Electric power applications, *IEE Proceedings B* , Vol.138, Issue. 5. Pp. 205-218, 1991.

[13] J. Puranen, "Induction Motor versus Permanent Magnet Synchronous Motor in Motion Control Applications: a comparative study", Dissertation, Lappeenranta University of Technology, Dec 2006.

[14] O.I. Okoro, "Dynamic and Thermal Modeling of Induction Machine with Non-Linear Effects", Dissertation Kassel University, Germany, 2002.

[15] R. Rothe, K. Hameyer, "Life Expectancy Calculation for Electric Vehicle Traction Motors Regarding Dynamic Temperature and Driving Cycles" , *IEEE International Conference on Electric Machines & Drives,* 2011.

[16] V.M. Montsinger, "Loading Transformers by temperature", *AIEETrans*. vol. 49, pp. 776-790, 1930.

[17] A.Boglietti, A. Cavagnino, "Analysis of the Endwinding Cooling Effects in TEFC Induction Motors", *IEEE Transactions on Industry Applications*, vol. 43, No.5, Sept. 2007.

[18] Standard IEC 61857-1, "Electrical Insulation Systems. Procedures for thermal evaluation- Part1: General requirements- Low voltage, 2008.

[19] D. Gerling, G.Dajaku "Novel lumped-parameter thermal model for electrical systems" *IEEE European Conference on Power Electronics and Applications*, 2005.

[20] Z.Gao, T. G. Habetler, R. G. Harley "An Online Adaptive Stator Winding Temperature Estimator Based on a Hybrid Thermal Model for Induction Machines", *IEEE International Conference on Electric Machines and Drives,* 2005.

[21] M.Hafner, M.Schöning, K. Hameyer "Automated Sizing of Permanent Magnet Synchronous Machines with respect to Electromagnetic and Thermal Aspects*", IEEE International Conference on Electrical Machines*, 2008.

[22] www.iem.rwth-aachen.de

BIOGRAPHIES

Sara Mahdavi received her Master degree in electrical power engineering from the Technical University of Darmstadt, Darmstadt, Germany. She has been working as a research associate at the Institute of Electrical Machines of RWTH Aachen University, Germany since May 2011. Her research interests include life time estimation, high frequency modeling as well as condition monitoring in electrical machines.

Thomas Herold was born in 1977 in Daun, Germany. He received the Dipl.-Ing. degree in electrical engineering from RWTH Aachen University, Aachen, Germany, in April 2007. After that he became a member of staff (research associate) at the Institute of Electrical Machines, RWTH Aachen University. Since 2010 he has been working as chief engineer of the institute. His main field of research is drive-train modeling and simulation, propulsion control, and system id entification.

Kay Hameyer (M'96-SM'99) received the M.Sc. degree in electrical engineering from the University of Hannover, Hannover, Germany, and the Ph.D. degree from the University of Technology Berlin, Berlin, Germany. After his university studies, he was with Robert Bosch GmbH, Stuttgart, Germany, as a Design Engineer for permanent-magnet servo motors and electrical board net components for vehicles. Until February 2004, he was a Full Professor of numerical field computations and electrical machines at the Katholieke Universiteit Leuven, Belgium. Since 2004 he is a Full Professor, the Director of the Institute of Electrical Machines, and the holder of the Chair Electromagnetic Energy Conversion at RWTH Aachen University, Aachen, Germany, where he has been the Dean of the Faculty of Electrical Engineering and Information Technology from 2007 to2009.

His research interests include numerical field computation and simulation, design of electrical machines, particularly permanent-magnet excited machines and induction machines, and numerical optimization strategies.